Table 2: Blood pressure, heart rate, and intraocular pressure in control and acupuncture therapy. The values represent the mean and SD. $^{*}P < .05$, $^{**}P < .01$ versus rest or before acupuncture. $^{\dagger}P < .05$, $^{\dagger\dagger}P < .01$ versus control.

Parameter	Control			Acupuncture		
	Rest	After 1 hour	Δ value	Before	After	Δ value
Systole blood pressure (mm Hg)	116.4 ± 10.0	119.8 ± 7.6	3.4 ± 7.4	124.5 ± 12.9	122.6 ± 9.7	−1.1 ± 7.9
Diastolic blood pressure (mm Hg)	69.8 ± 6.5	68.6 ± 3.9	−1.0 ± 9.4	74.5 ± 5.4	72.0 ± 2.9	−3.0 ± 5.5
Heart rate (beats/min)	61.5 ± 7.3	60.1 ± 8.1	−2.5 ± 3.8	61.7 ± 8.5	60.3 ± 10.4	−2.4 ± 5.5
Intraocular pressure (mm Hg)	16.0 ± 4.1	17.1 ± 4.2**	1 ± 0.9	17.0 ± 5.0	16.0 ± 4.3*	−1 ± 1.9††

Table 3: Resistive index (RI) in the ophthalmic artery, central retinal artery, and short posterior ciliary artery. The values represent the mean and SD. $^{*}P < .05$, $^{**}P < .01$ versus before acupuncture. $^{\dagger}P < .05$, $^{\dagger\dagger}P < .01$ versus control.

Resistive index	Control			Acupuncture		
	Rest	After 1 hour	Δ value	Before	After	Δ value
Ophthalmic artery	0.74 ± 0.04	0.75 ± 0.05	0.006 ± 0.037	0.74 ± 0.04	0.74 ± 0.04	−0.006 ± 0.036
Central retinal artery	0.75 ± 0.09	0.72 ± 0.03	−0.027 ± 0.085	0.72 ± 0.05	0.68 ± 0.04*	−0.036 ± 0.059
Short posterior ciliary artery	0.68 ± 0.05	0.68 ± 0.04	0.004 ± 0.038	0.67 ± 0.04	0.64 ± 0.06*	−0.032 ± 0.054††

significantly by acupuncture compared with before acupuncture ($P < .05$). The Δ value of RI in the SPCA also significantly decreased by acupuncture compared with control ($P < .01$) (Table 3).

5. Discussion

To our best knowledge, this is the first report on hemodynamic change in retrobulbar vessels related to acupuncture in OAG eyes. The present findings suggest that acupuncture can alter vessel resistance in the SPCA, even though the eyes are treated with standard medications.

The OA originates from the internal carotid artery. The CRA and SPCA are the ocular branches of the OA [32]. The CRA supplies blood to the retina and SPCA, to the choroid. CDI by ultrasound is useful for the measurement of the blood flow in various vessels in real time. Since it is impossible to determine the diameter of very small retrobulbar vessels, CDI cannot directly measure blood flow volume. However, the decrease of the distal vascular resistance in the SPCA indicates an increase of the blood flow in the choroid. We have already reported that acupuncture could increase the blood flow volume in the upper limb without an increase in the cardiac output, and the increased reaction in the blood flow was mediated by the decrease in the vascular resistance on the basis of the decreased vascular tone [30]. The mechanisms by which acupuncture can alter retrobulbar vessel circulation are still unclear. However, it has been reported that the blood flow in the eye is controlled by sympathetic and parasympathetic nerves, and it is related with the release of nitric oxide or calcitonin gene-related peptide [33, 34]; it has also been reported that the regulation of regional blood flow by somatic afferent stimulation is based on somatoautonomic reflex mechanisms in the choroidal blood flow of the eyeball [34]. The hemodynamic changes in the SPCA by acupuncture may be related with these mechanisms. Reduced blood flow velocities and increased vascular resistance in the retrobulbar arteries appear to be a risk factor for glaucoma progression [35–38]. Thus, acupuncture may be applied for additional therapy to treat OAG.

We should view these results cautiously because the present study was a case series study and intervention was provided only once. Longer observation of acupuncture therapy is needed to investigate the progression of glaucomatous damage associated with impaired ocular circulation.

6. Conclusions

The vessel resistance in the SPCA and the IOP level were decreased by acupuncture in OAG eyes. Acupuncture can affect the retrobulbar circulation and IOP despite the administration of standard medication. The present study implies the possibility that acupuncture is effective for OAG with standard medication.

Acknowledgment

This work was supported by Health and Labour Sciences Research Grants for Clinical Research from the Japanese Ministry of Health, Labour and Welfare.

References

[1] K. Nakae, K. Masuda, T. Aneo et al., "Wagakuni ni okeru shiryokushougai no genjou," *Research Committee on Chorioretinal Degenerations and Optic Atrophy, the Ministry of Health, Labour and Welfare of Japan*, vol. 17, pp. 263–276, 2005.

[2] A. Iwase, Y. Suzuki, M. Araie et al., "The prevalence of primary open-angle glaucoma in Japanese: the Tajimi study," *Ophthalmology*, vol. 111, no. 9, pp. 1641–1648, 2004.

[3] R. N. Weinreb and P. Tee Khaw, "Primary open-angle glaucoma," *The Lancet*, vol. 363, no. 9422, pp. 1711–1720, 2004.

[4] C. Akarsu and M. Y. K. Bilgili, "Color Doppler imaging in ocular hypertension and open-angle glaucoma," *Graefe's*

Archive for Clinical and Experimental Ophthalmology, vol. 242, no. 2, pp. 125–129, 2004.

[5] V. P. Costa, A. Harris, E. Stefánsson et al., "The effects of antiglaucoma and systemic medications on ocular blood flow," *Progress in Retinal and Eye Research*, vol. 22, no. 6, pp. 769–805, 2003.

[6] H. J. Kaiser, A. Schoetzau, D. Stumpfig, and J. Flammer, "Blood-flow velocities of the extraocular vessels in patients with high- tension and normal-tension primary open-angle glaucoma," *American Journal of Ophthalmology*, vol. 123, no. 3, pp. 320–327, 1997.

[7] S. J. A. Rankin, "Color Doppler imaging of the retrobulbar circulation in glaucoma," *Survey of Ophthalmology*, vol. 43, no. 1, pp. S176–S182, 1999.

[8] I. Stalmans, A. Harris, S. Fieuws et al., "Color Doppler imaging and ocular pulse amplitude in glaucomatous and healthy eyes," *European Journal of Ophthalmology*, vol. 19, no. 4, pp. 580–587, 2009.

[9] I. Janulevičiene, I. Sliesoraityte, B. Siesky, and A. Harris, "Diagnostic compatibility of structural and haemodynamic parameters in open-angle glaucoma patients," *Acta Ophthalmologica*, vol. 86, no. 5, pp. 552–557, 2008.

[10] N. Plange, M. Kaup, O. Arend, and A. Remky, "Asymmetric visual field loss and retrobulbar haemodynamics in primary open-angle glaucoma," *Graefe's Archive for Clinical and Experimental Ophthalmology*, vol. 244, no. 8, pp. 978–983, 2006.

[11] M. Satilmis, S. Orgül, B. Doubler, and J. Flammer, "Rate of progression of glaucoma correlates with retrobulbar circulation and intraocular pressure," *American Journal of Ophthalmology*, vol. 135, no. 5, pp. 664–669, 2003.

[12] J. Schumann, S. Orgül, K. Gugleta, B. Dubler, and J. Flammer, "Interocular difference in progression of glaucoma correlates with interocular differences in retrobulbar circulation," *American Journal of Ophthalmology*, vol. 129, no. 6, pp. 728–733, 2000.

[13] Y. Yamazaki and S. M. Drance, "The relationship between progression of visual field defects and retrobulbar circulation in patients with glaucoma," *American Journal of Ophthalmology*, vol. 124, no. 3, pp. 287–295, 1997.

[14] X. Xu, "Acupuncture in an outpatient clinic in China: a comparison with the use of acupuncture in North America," *Southern Medical Journal*, vol. 94, no. 1-10, pp. 813–816, 2001.

[15] V. Napadow and T. J. Kaptchuk, "Patient characteristics for outpatient acupuncture in Beijing, China," *Journal of Alternative and Complementary Medicine*, vol. 10, no. 3, pp. 565–572, 2004.

[16] C. M. Witt, S. Jena, B. Brinkhaus, B. Liecker, K. Wegscheider, and S. N. Willich, "Acupuncture for patients with chronic neck pain," *Pain*, vol. 125, no. 1-2, pp. 98–106, 2006.

[17] B. Brinkhaus, C. M. Witt, S. Jena et al., "Acupuncture in patients with chronic low back pain: a randomized controlled trial," *Archives of Internal Medicine*, vol. 166, no. 4, pp. 450–457, 2006.

[18] D. Melchart, A. Streng, A. Hoppe et al., "Acupuncture in patients with tension-type headache: randomised controlled trial," *British Medical Journal*, vol. 331, no. 7513, pp. 376–379, 2005.

[19] C. Witt, B. Brinkhaus, S. Jena et al., "Acupuncture in patients with osteoarthritis of the knee: a randomised trial," *The Lancet*, vol. 366, no. 9480, pp. 136–143, 2005.

[20] K. Linde, A. Streng, S. Jürgens et al., "Acupuncture for patients with migraine: a randomized controlled trial," *Journal of the American Medical Association*, vol. 293, no. 17, pp. 2118–2125, 2005.

[21] *Diseases of Eyes, Ears, Nose and Throat*, vol. 681, Eastland Press, Seattle, Wash, USA, 1981.

[22] M. Kurusu, K. Watanabe, T. Nakazawa et al., "Acupuncture For Patients With Glaucoma," *Explore*, vol. 1, no. 5, pp. 372–376, 2005.

[23] S. Naruse, K. Mori, M. Kurihara et al., "Chorioretinal blood flow changes following acupuncture between thumb and forefinger," *Journal of Japanese Ophthalmological Society*, vol. 104, no. 10, pp. 717–723, 2000.

[24] M. Shimura, S. Uchida, A. Suzuki, K. Nakajima, and Y. Aikawa, "Reflex choroidal blood flow responses of the eyeball following somatic sensory stimulation in rats," *Autonomic Neuroscience*, vol. 97, no. 1, pp. 35–41, 2002.

[25] J. J. Steinle, D. Krizsan-Agbas, and P. G. Smith, "Regional regulation of choroidal blood flow by autonomic innervation in the rat," *American Journal of Physiology*, vol. 279, no. 1, pp. R202–R209, 2000.

[26] S. Takayama, T. Seki, N. Sugita et al., "Radial artery hemodynamic changes related to acupuncture," *Explore*, vol. 6, no. 2, pp. 100–105, 2010.

[27] S. Takayama, T. Seki, M. Watanabe et al., "Changes of blood flow volume in the superior mesenteric artery and brachial artery with abdominal thermal stimulation," *Evidence-Based Complementary and Alternative Medicine*, vol. 17, pp. 1–9, 2009.

[28] S. Takayama, T. Seki, M. Watanabe et al., "The herbal medicine Daikenchuto increases blood flow in the superior mesenteric artery," *Tohoku Journal of Experimental Medicine*, vol. 219, no. 4, pp. 319–330, 2009.

[29] S. Takayama, T. Seki, M. Watanabe et al., "The effect of warming of the abdomen and of herbal medicine on superior mesenteric artery blood flow—a pilot study," *Forschende Komplementarmedizin*, vol. 17, no. 4, pp. 195–201, 2010.

[30] S. Takayama, T. Seki, M. Watanabe et al., "Brief effect of acupuncture on the peripheral arterial system of the upper limb and systemic hemodynamics in humans," *Journal of Alternative and Complementary Medicine*, vol. 16, no. 7, pp. 707–713, 2010.

[31] E. T. Matthiessen, O. Zeitz, G. Richard, and M. Klemm, "Reproducibility of blood flow velocity measurements using colour decoded Doppler imaging," *Eye*, vol. 18, no. 4, pp. 400–405, 2004.

[32] S. S. Hayreh and R. Dass, "The ophthalmic artery II: intra orbital course," *The British Journal of Ophthalmology*, vol. 46, no. 3, pp. 165–185, 1962.

[33] A. K. Wiencke, H. Nilsson, P. J. Nielsen, and N. C. B. Nyborg, "Nonadrenergic noncholinergic vasodilation in bovine ciliary artery involves CGRP and neurogenic nitric oxide," *Investigative Ophthalmology and Visual Science*, vol. 35, no. 8, pp. 3268–3277, 1994.

[34] M. Shimura, S. Uchida, A. Suzuki, K. Nakajima, and Y. Aikawa, "Reflex choroidal blood flow responses of the eyeball following somatic sensory stimulation in rats," *Autonomic Neuroscience*, vol. 97, no. 1, pp. 35–41, 2002.

[35] D. Gherghel, S. Orgül, K. Gugleta, M. Gekkieva, and J. Flammer, "Relationship between ocular perfusion pressure and retrobulbar blood flow in patients with glaucoma with progressive damage," *American Journal of Ophthalmology*, vol. 130, no. 5, pp. 597–605, 2000.

[36] O. Zeitz, P. Galambos, L. Wagenfeld et al., "Glaucoma progression is associated with decreased blood flow velocities in the short posterior ciliary artery," *British Journal of Ophthalmology*, vol. 90, no. 10, pp. 1245–1248, 2006.

[37] F. Galassi, A. Sodi, F. Ucci, G. Renieri, B. Pieri, and M. Baccini, "Ocular hemodynamics and glaucoma prognosis: a color Doppler imaging study," *Archives of Ophthalmology*, vol. 121, no. 12, pp. 1711–1715, 2003.

[38] A. Martínez and M. Sánchez, "Predictive value of colour Doppler imaging in a prospective study of visual field progression in primary open-angle glaucoma," *Acta Ophthalmologica Scandinavica*, vol. 83, no. 6, pp. 716–722, 2005.

Displays 32 (2011) 201–208

Contents lists available at ScienceDirect

Displays

journal homepage: www.elsevier.com/locate/displa

Evaluation of temporal relationship between a physiological index and a subjective score using average mutual information

Norihiro Sugita [a,*], Makoto Yoshizawa [b], Akira Tanaka [c], Makoto Abe [b], Noriyasu Homma [b], Shigeru Chiba [d], Tomoyuki Yambe [e], Shin-ichi Nitta [e]

[a] Graduate School of Engineering, Tohoku University, 6-6-05 Aoba, Aramaki, Aoba-ku, Sendai 980-8579, Japan
[b] Information Synergy Center, Tohoku University, 6-6-05 Aoba, Aramaki, Aoba-ku, Sendai 980-8579, Japan
[c] Faculty of Symbiotic Systems Science, Fukushima University, 1 Kanayagawa, Fukushima 960-1296, Japan
[d] Sharp Corporation, 1-9-2 Nakase, Mihama-ku, Chiba 261-8520, Japan
[e] Institute of Development, Aging and Cancer, Tohoku University, 4-1 Seiryo-machi, Aoba-ku, Sendai 980-8575, Japan

ARTICLE INFO

Article history:
Available online 15 May 2011

Keywords:
Visually-induced motion sickness
Physiological index
Subjective score
Averaged mutual information

ABSTRACT

Recently, because of the ubiquitous popularization of home video cameras, countless people have had opportunities to watch video images captured by amateur cameramen. Because of this, concerns have arisen over potential negative impacts on viewer health, such as visually-induced motion sickness (VIMS). To determine the mechanism inducing VIMS and to establish a method of preventing it, it is necessary to understand which types of video scenes are associated with the onset of VIMS. Furthermore, while it is useful to consider viewer self-assessments while watching such scenes, physiological indices can provide even more information because they can be measured second-by-second in real time. However, there is not much knowledge regarding the temporal relationships between the severity of VIMS and its accompanying physiological conditions. In this study, the average mutual information was employed to determine the temporal relationship between subjective evaluation scores (a subject's personal evaluation of his/her own condition) and various physiological indices present when people suffer from VIMS. Our analysis of experimental data found that changes in the two physiological indices, which were respiratory sinus arrhythmia and the maximum cross-correlation coefficient between heart rate and pulse transmission time, had a concordance rate of more than 60% with changes in the severity of VIMS symptoms experienced by test subjects. Furthermore, we determined that it may be possible to detect signs of impending VIMS prior to the development of symptoms by analyzing physiological indices.

1. Introduction

In recent years, countless people have seen moving video images taken by amateur videographers. As a consequence, video cameras have become significantly less expensive and because the popular trend of posting private videos on the Internet has expanded exponentially. Concurrently, the number of cases reported in which viewers suffered from visually-induced motion sickness (VIMS) during or after watching a video, including unexpected whole image motion and vibration [1–9], has increased. VIMS is a form of motion sickness that does not require the subject to experience motion. However, VIMS symptoms are similar to those of other motion sicknesses. Most notably, such symptoms include skin pallor, excessive perspiration, nausea, and vomiting. At a junior high school in Japan on July 10, 2003, an incident occurred in which 36 of 294 students were treated in a hospital after complaining of dizziness and nausea induced by watching a video taken by an amateur videographer with a swaying handheld camera [6]. Furthermore, several film distributors and video game producers have recently issued warnings to viewers or users about the possibility of experiencing VIMS from watching their videos or playing their games: a movie titled "Clover Field" released in 2008 was one such example.

A number of *hypotheses* and discussions about the pathogenesis of various forms of motion sickness, including VIMS [10–12], have been explored. Nevertheless, there is currently little understanding about adverse effects of VIMS on the human body. Accordingly, sufficient attention should be focused on dealing with moving images and scenes that have potential to induce VIMS, especially in the case of children, because their nervous systems are immature.

To isolate the VIMS induction mechanism and to establish a method of preventing it, it is important to understand which

* Corresponding author. Tel.: +81 22 7957130; fax: +81 22 2639163.
E-mail address: sugita@yoshizawa.ecei.tohoku.ac.jp (N. Sugita).

0141-9382/$ - see front matter © 2011 Elsevier B.V. All rights reserved.
doi:10.1016/j.displa.2011.04.003

scenes in a video are associated with the onset of VIMS. Self-assessment of VIMS by subjects at regular intervals is considered to be one of the most effective methods of detecting these scenes. In particular, Kennedy developed the Simulator Sickness Questionnaire (SSQ) [13] which has been used in many studies [14–17]. The SSQ contains 16 items to check the subject's physical disorder. The subject rates the degree of these items in four levels. Three subscales, i.e., nausea, oculomotor, and disorientation, are calculated on the basis of these items, and a total score is calculated with these subscales. In these scales, the nausea subscale or the total score is considered to be useful for evaluating the severity of VIMS. However, since SSQ results can normally only be obtained after a subject has watched a video, it is difficult to follow changes in VIMS severity over time. Furthermore, even if self-assessment is accomplished using an easier reporting method than SSQ, such as reporting symptoms via keyboard input or verbally, the very act of making such reports has the potential to distract subjects from the scene they are viewing, and thus modify the VIMS development.

In contrast, other previous studies [2–5,7,8,18–23] have reported that real-time monitoring of physiological indices is also useful for detecting and following the development of VIMS. Specifically, skin conductance [20,21] and gastric tachyarrhythmia [2,20,22] are considered to be particularly indicative of possible VIMS. Furthermore, physiological indices based on heart rate variability (HRV) such as variations in respiratory sinus arrhythmia (RSA) [10,11] have possibilities of detecting the development of VIMS. The indices obtained from HRV are associated with autonomic nervous activity. Fig. 1 shows an example of the power spectrum density of HRV. In this figure, the high frequency component corresponding to RSA includes parasympathetic nervous activity only while the low frequency component (LF_{HRV}) includes both sympathetic and parasympathetic nervous activities [24,25]. These physiological indices are susceptible to change when a person experiences VIMS because VIMS is considered to be a kind of the physical and emotional stress which disturbs autonomic nervous balance. We previously proposed a maximum cross-correlation coefficient (ρ_{max}) between heart rate and blood pressure and reported that this index decreased significantly when people suffered from VIMS [4]. ρ_{max} is considered to reflect baroreflex function which is influenced by autonomic nervous activity [26–28]. In addition, ρ_{max} which was calculated using pulse transmission time (PTT) [29] instead of blood pressure was also found to be useful when evaluating VIMS effects [3,5].

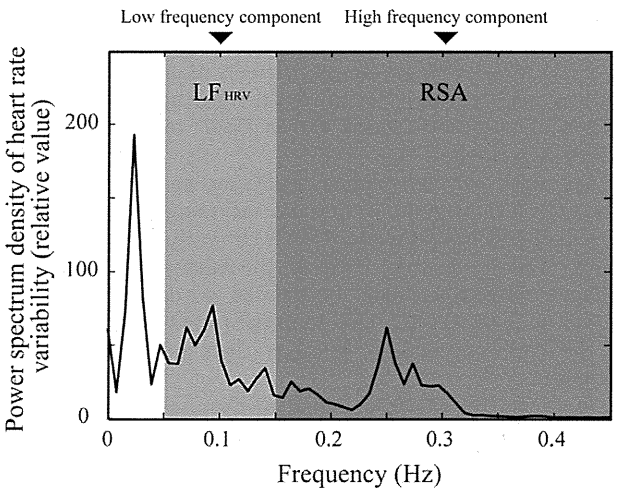

Fig. 1. The power spectrum density of heart rate variability.

Information on the abovementioned physiological indices can be obtained in real-time using non-invasive sensors while the subjects are watching a video, which makes it possible to compare changes in these indices with particular video scenes and thus observe the process of VIMS onset with relatively little effect on the subjects. However, one problem identified is that biological reaction times, especially response times, vary between individuals. Meanwhile, there have been few studies into the temporal relationship between the development of VIMS as evaluated by subjective scores and by the physiological responses of the subjects [19].

In this study, we hypothesize that there is no significant difference between the time when subjects experience VIMS symptoms and the time when their physiological states change. To test this hypothesis, an experiment was conducted to investigate the temporal relationship between a subjective score and four physiological indices, HRV, LF_{HRV}, RSA, and ρ_{max}, from subjects experiencing VIMS. It was not clear whether HRV and LF_{HRV} reflect the development of VIMS, although RSA and ρ_{max} were reported to have relationships with VIMS in previous works [3–5,18,19].

2. Methods

2.1. Experimental design

In the experimental phase of this study, both subjective scores and biological signals were measured simultaneously while subjects were watching a video. The test subjects evaluated the degrees of VIMS they experienced at regular intervals using a joystick. In contrast, physiological state changes, HRV, LF_{HRV}, RSA, and ρ_{max} using PTT were obtained via biological signals, and were used as physiological indices to test our hypothesis. Furthermore, we proposed a new evaluation indicator, which will be described in detail later, to investigate the temporal relationship between subjective scores and the physiological indices.

The experimental protocol was approved by the University's Internal Review Board.

2.2. Participants

Fifty-one adults (22 males and 29 females; 26.6 ± 9.3 years) participated in the experiment. They were recruited via posted announcements on university notice boards, and all of them received payment for their participation in the experiment.

Informed consent was obtained from each of the subjects and each was asked about their backgrounds and health conditions through a questionnaire. The results of the questionnaire showed that there were no test subjects whose participation in the experiment would be unsuitable due to health issues.

2.3. Stimulus

The subjects watched a 20-min-long amateur video that included three segments, as shown in Fig. 2. Segment one consisted of moving images taken by a young girl using a hand-held camera while strolling around an urban area. Therefore, the video contained numerous scenes that included unexpected whole image motions and vibration. The images of Segment 2 were taken in an amusement park. Thus, the camera movements were sometimes intense due to the movements of the theme-park rides. Segment 3 includes images of a young woman strolling around a city, recorded normally, and using four simple camera motions: tilt, pan, roll and zoom. Before and after these segments, a gray, imageless screen display was presented to the subjects for 5 min 30 s and 2 min, respectively. Therefore, each subject watched a total of 27 min 30 s of video during the experiment. None of the three vi-

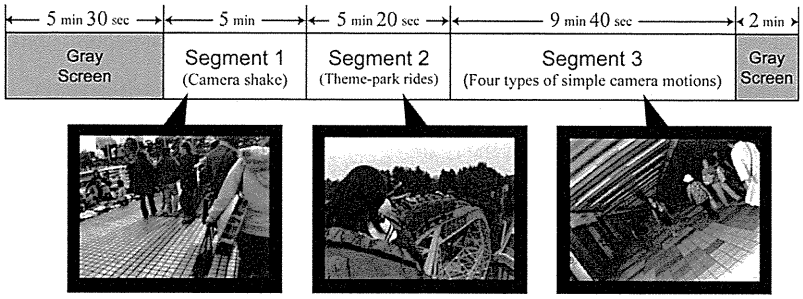

Fig. 2. Overview of the video presented to experimental subjects.

deo segments had story lines and there were no violent scenes that might induce emotional effects.

The global motion vectors (GMVs) of the video are shown in Fig. 6a). GMVs are measurements of deviation between consecutive frames and represent degrees of motions in four axes: pan, tilt, roll and zoom. A detailed description of the method used for estimating GMVs is provided in Ref. [30]. As shown in Fig. 6a, scenes with intense camera movements and those without were mixed in the video on purpose to induce ups and downs of VIMS symptoms.

2.4. Equipment

The video was shown on a 37-in. liquid crystal display (resolution: 1920 × 1080 pixels, maximum brightness: 200 cd/m^2). The experimental room had curtains that eliminated all outside light and illumination intensity was maintained at approximately 50 l×. The room temperature was controlled with an air conditioner to be approximately 22 °C.

During the experiment, an electrocardiogram (ECG) for RSA, PTT, and HRV was measured using electrodes placed on the subjects chests. In addition, a finger photoplethysmogram (PPG) for PTT was also measured using a photoplethysmographic sensor attached on their finger tips, as shown in Fig. 3. These signals were amplified and recorded by a data acquisition system (MP-100, ECG100C, PPG100C; BIOPAC System Inc.); whose voltage resolution and sampling rate were 16 bit and 1 kHz, respectively.

2.5. Procedure

The subjects were instructed not to engage in intense physical activity and to avoid eating anything for 2 h prior to the experiment.

First, each subject was asked to complete a questionnaire about their background and health condition. Additionally, an SSQ [13] was administered before and after the experimental task to measure their VIMS symptoms. Next, after being seated in the room and given 10 min to adapt to the darkness, they began viewing the video.

While watching the video, test subjects sat on a chair placed 70 cm away from the display with a 60.5 × 40.3° field of view, and they rated the level of nausea they felt on a scale of zero to three by moving a joystick, as shown in Fig. 4. The number of symptom levels was limited to four and enough time for practice was given to the subjects before the experiment so that they could move the joystick appropriately without looking at it. A buzzer was sounded at 1 min intervals to let the subjects know it was time to rate their nausea level.

2.6. Data analysis

There were five subjects who complained of VIMS symptoms that were so severe that they could not continue to watch the video. All these subjects experienced nausea and had unnatural skin pallor. One female test subject developed an erratic heartbeat just before the experiment was stopped. Additionally, test data from 17 other subjects were excluded from the analysis because of artifacts. There were a large number of subjects whose photoplethysmogram signals contained artifacts caused by body movements. As shown in Fig. 3, the photoplethysmographic sensor is attached to the skin on a finger of a subject and detects infrared light modulated by blood pulsing through the tissue below. Therefore, the photoplethysmogram signal is disturbed if the subject's upper body including fingers moves much. Furthermore, data from another six subjects whose subjective scores were zero through the video were also excluded from the analysis. The reason of this will be discussed later. As a result, only the data of 23 subjects (10 males and 13 females; 27.6 ± 10.0 years) were analyzed.

As previously mentioned, we proposed a new evaluation indicator to investigate the temporal relationship between subjective

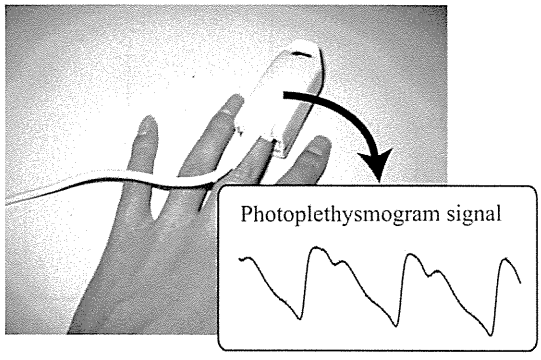

Fig. 3. Photoplethysmographic sensor attached on a subject's finger tips.

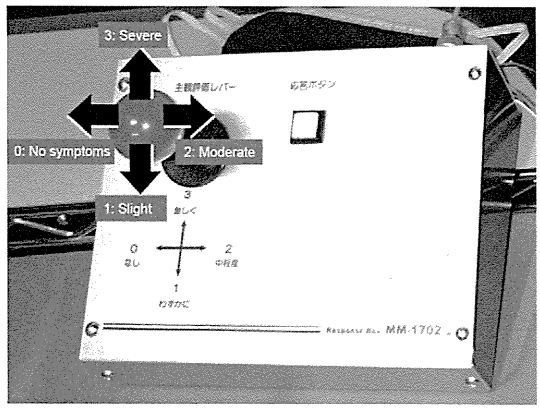

Fig. 4. Joystick used by subjects to rate VIMS symptoms during the experiment.

scores and physiological indices. In concrete terms, the average mutual information (AMI) [31] was calculated to measure the statistical dependence between the two. The AMI between two variables shows how frequently, on average, one of them can be estimated from the other. Thus, by introducing the AMI, it is possible to estimate the statistical dependence correctly even if the relationship between the variables is not linear. This property is important because our understanding of the linearity between subjective scores and physiological indices is still poor.

Problems sometimes occurred when calculating the AMI between subjective scores and physiological indices. Specifically, not only is the difference in the numeric resolution between them large, but the pattern of their changes differs significantly between individual subjects. To solve these problems, the AMI was calculated as the statistical dependence between events defined by changing patterns of variables, which were assessed as increasing, decreasing or stable.

We will further illustrate this point with an example utilizing two test subjects. In this example, when the subjective scores of the two subjects increase, the physiological index of one subject always increases while that of the other always decreases, and vice versa. In this situation, a difference appears in the value of an AMI calculated directly from the physiological index and the subjective scores of the two subjects. In contrast, the value of an AMI calculated based on events defined by changing patterns of the physiological index and the subjective scores of the two subjects is the same. Types of VIMS symptoms should differ among subjects, for example, eye fatigue, a headache or stomach discomfort. And autonomic nervous activities are supposed to vary in these different symptoms. For this reason, it is no wonder if directions of the change in physiological indices differ among the subjects when they suffered from VIMS. Additionally, the problem caused by the numerical differences between the two variables is also eliminated by simply comparing their changing patterns.

The method used to calculate the AMI will now be described in detail. First, events A_1, A_2, A_3 and B_1, B_2, B_3 are defined as follows:

$$\begin{aligned} A_1 &\Longleftrightarrow SS(k) - SS(k-1) > 0 \\ A_2 &\Longleftrightarrow SS(k) - SS(k-1) = 0 \\ A_3 &\Longleftrightarrow SS(k) - SS(k-1) < 0 \end{aligned} \tag{1}$$

$$\begin{aligned} B_1 &\Longleftrightarrow \frac{PS(k)}{PS(k-1)} > 1 + Tr \\ B2 &\Longleftrightarrow 1 - Tr < \frac{PS(k)}{PS(k-1)} \leqslant 1 + Tr \\ B3 &\Longleftrightarrow \frac{PS(k)}{PS(k-1)} \leqslant 1 - Tr \end{aligned} \tag{2}$$

where $SS(k)$ and $PS(k)$ are the subjective score and the physiological index at a given time k, respectively, and Tr is the threshold. A method to determine Tr is described later.

Next, the AMI between A_i and B_j (i, $j = 1,2,3$) is defined as follows:

$$I(A_i; B_j) = -\sum_{i=1}^{3} P(A_i)\log_2 P(A_i) + \sum_{i=1}^{3}\sum_{j=1}^{3} P(A_i, B_j)\log_2 P(A_i|B_j) \tag{3}$$

where $P(A_i)$ is the occurrence probability of A_i, $P(A_i, B_j)$ is the joint probability of A_i and B_j, and $P(A_i|B_j)$ is the conditional probability of A_i assuming that B_j has occurred.

By its nature, I between arbitrary variables X and Y does not contain directional information. In other words, I does not show causality between X and Y, although it is possible to detect causality between X and Y by the calculation of I using X_L instead of X. X_L is the time series which lags X by L [32]. That is, I between $SS(k)$ and $PS(k + L)$, which is denoted as $I(L)$, shows how much time lag or lead there is between physiological and psychological state changes. $I(L)$ was calculated under lag time set from $L = -2$ to 2 min.

To determine the value of the threshold Tr in equation (2), an assessment function $H(Tr)$ is defined as follows:

$$H(Tr) = \max_{-2 \leqslant L \leqslant 2} I(L) \tag{4}$$

For each subject, the value of Tr was selected to maximize $H(Tr)$ in the range from $Tr = 0.01$ to 0.15.

In this study, the subjective score obtained from the joystick input was chosen as $SS(k)$. Meanwhile, time series of ρ_{max} using PTT, RSA, HRV and LF_{HRV} were chosen as $PS(k)$.

In order to obtain time series of these parameters, beat-to-beat data of HRV and PTT were first calculated. The HRV was calculated from the reciprocal of the inter-R-wave interval of ECG signal and the PTT was defined as the interval from the peak of ECG, R-wave, to the point at which PPG signal begins to rise. And then, at a given time k (min), $\rho_{max}(k)$ was calculated based on the HRV and the PTT observed in the interval between $k - 1$ and k (min). A detailed description of the calculation method of ρ_{max} is provided in Ref. [5]. Similarly, $HRV(k)$, $LF_{HRV}(k)$ and $RSA(k)$ were calculated as the mean value, the low-frequency power (0.05–0.15 Hz) and the high-frequency power (0.15–0.45 Hz) of HRV, respectively, in the same interval as described above.

3. Results

Fig. 5 shows the results of the SSQ completed by the subjects before and after the experiment. In these results, all SSQ scores increased significantly ($p < 0.01$, paired t-test) after watching the video and got closer to those obtained from the subjects who were suffered from cyber sickness or simulator sickness [14,23]. Therefore, the moving images included in the video are considered to have induced VIMS.

Fig. 6b shows the changes in ρ_{max} and SS of a subject. SS increased at 11, 15, 20, 24 and 26 min, while ρ_{max} decreased at approximately the same points of time (except for the 24 min point). Fig. 6c shows the average mutual information I between SS and ρ_{max} of this subject. In this figure, I at $L = 0$ min was higher than those observed at the other lag times. This result indicates that the subject's physiological state changed at approximately the same time a VIMS sensation was experienced.

From Fig. 6c, I had a value of 0.3 at $L = 0$. However, the meaning of this value is unclear. Therefore, a computer simulation was carried out to investigate the relationship between I and the concor-

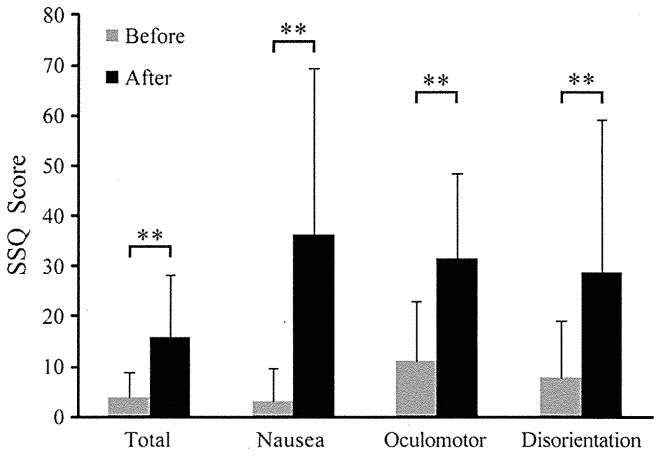

Fig. 5. SSQ scores obtained from subjects before and after watching the video. **$p < 0.01$, paired t-test.

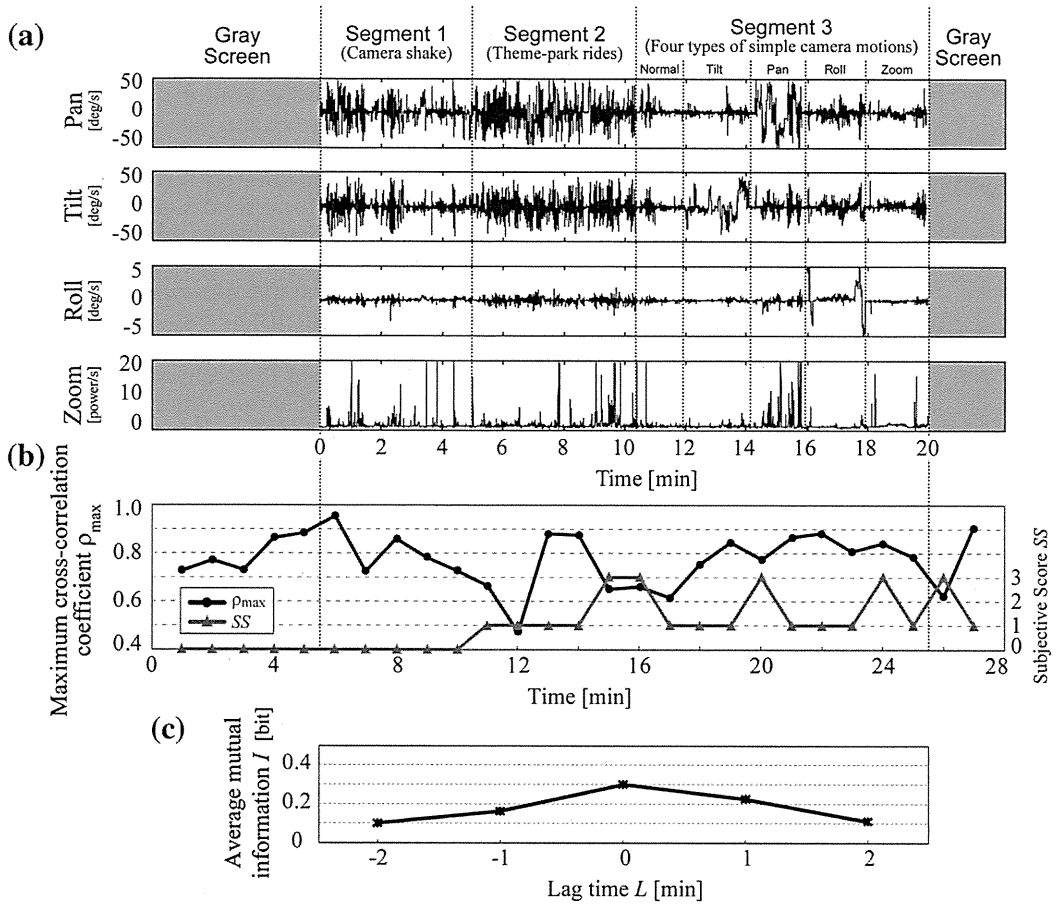

Fig. 6. (a) The global motion vectors of the self-produced video, (b) changes in ρ_{max} (black line) and *SS* (gray line) of a subject, and (c) average mutual information *I* between the *SS* and the ρ_{max}.

dance rate p_c of changing patterns of two temporal sequences resembling $SS(k)$ and $PS(k)$. In the simulation, these temporal sequences changed in the same direction at a rate of p_c (%) and did so in random directions at a rate of 100 – p_c (%).

Fig. 7 shows the simulation results. The curve shown in the figure was obtained from a simulation that was performed 1000 times. It can be seen that *I* had a minimum value when p_c was about 33%. This is because there were only three events defined by the difference in the changing pattern of temporal sequences, as shown in Eqs. (1) and (2). Therefore, even if changes to these temporal sequences are perfectly random and there is no statistical dependence between them, they change in the same direction, at a minimum, 33% of the time. This result implies that it is meaningless to compare the values of *I* which are lower than 0.15. In addition, there was a tendency in *I* to increase as p_c decreases when p_c was lower than 33%. This is because the occurrence of two temporal sequences whose changing patterns are significantly different to each other is extremely unlikely to be coincidental.

Fig. 8 shows the mean values of *I* between *SS* and ρ_{max}. These values were calculated as the mean of all test subjects with respect to each lag time between $L = -2$ and 2 min. The values of *I* at $L = -2$ and 2 min showed a lower level than those at the other lag times. However, the standard deviation of *I*, which means individual differences, was high for all lag times. In Fig. 9, relationships between lag time and *I* were plotted for all the subjects whose *I* were the highest at $L = -1$ or 1, hereinafter referred to as $L_{max} = -1$ or 1, respectively. As shown in this figure, there is a possibility that each subject has his/her specific L_{max} because there is only one peak in *I* of each subject for all lag times. And the values of *I* were less than

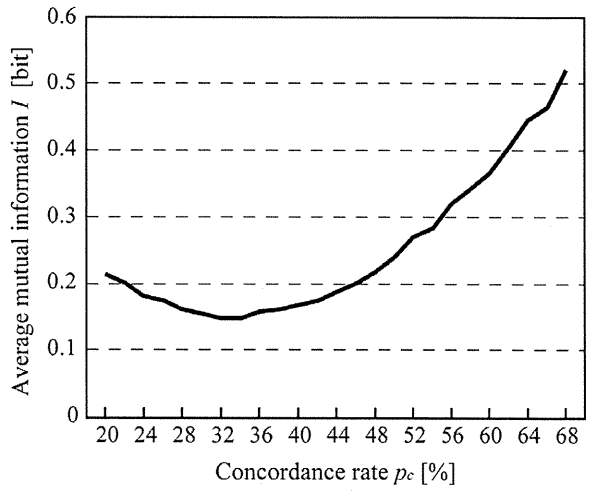

Fig. 7. Relationship between average mutual information *I* and the concordance rate p_c of changes in temporal sequences resembling $SS(k)$ and $PS(k)$. This is the simulation result.

0.2 at other lag times than L_{max}, which indicates there is no statistical dependence between *PS* and *SS*. Thus, for example, if the number of subjects whose L_{max} were −1 increases, the mean value of *I* at $L = 1$ will be relatively low.

To investigate not only the distribution but also the mean value of *I* for subjects with different L_{max}, the mean value of *I* at a lag time L_0 was only calculated for subjects whose L_{max} were L_0. For exam-

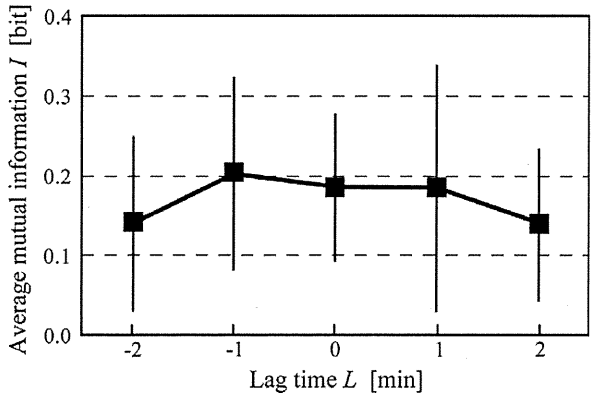

Fig. 8. The mean values of the average mutual information I between SS and ρ_{max}. These values were calculated as the mean of all the subjects with respect to each lag time between $L = -2$ and 2 min.

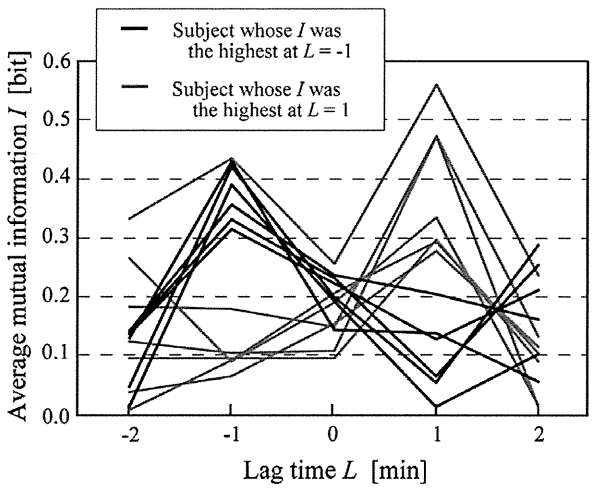

Fig. 9. The average mutual information I between SS and ρ_{max} of individual subjects whose I was the highest at $L = -1$ (black line) or $L = 1$ (gray line).

ple, the mean value of I at $L = -1$ was only calculated for six subjects whose I was the highest at $L = -1$ for all lag times.

Fig. 10 shows relationships between lag time L and the mean values of I calculated from four physiological indices: (a) ρ_{max}, (b) *RSA*, (c) *HRV* and (d) LF_{HRV}. These mean values run from 0.1 through 0.4. Also, as shown in Fig. 10a, the values of I obtained from ρ_{max} were higher and standard deviations were lower compared to the results shown in Fig. 8.

In Fig. 10a, I of ρ_{max} was relatively high both at $L = -1$ and 1 and the standard deviation was small, especially at $L = -1$. Additionally, the values of I for *HRV* and LF_{HRV} were lower than that of ρ_{max} on the whole, as shown in Fig. 10c and d. In contrast, for *RSA* shown in Fig. 10b, I was relatively high and the standard deviation was small at $L = 0$.

The statistical significances of the mean values of I among lag times were tested by one-way ANOVA for ρ_{max}, *RSA*, *HRV* and LF_{HRV}. However, no significant difference was found, except for LF_{HRV}. Significant differences were found in the values of I for LF_{HRV} between $L = -2$ and -1, and between $L = -1$ and 1 ($p < 0.05$, Tukey–Kramer test).

4. Discussion

As mentioned in the Methods section, data from six subjects whose subjective scores, *SS*, were zero through the video were excluded from the analysis. The equation of AMI, equation (3), implies that $I(L)$ is always zero for any lag time L if all *SS* are zero. This means that it is impossible to know the temporal relationship between the subjective evaluation scores and physiological indices of the six subjects because their L_{max} are indeterminate.

From Fig. 10, it can be seen that the values of I that were obtained for ρ_{max} and *RSA* were higher than those for the other physiological indices. These results agree with other studies that show that changes in these indices had a relationship to the development of motion sickness [3,5,18,19,17]. The mean value of I obtained for ρ_{max} and *RSA* was about 0.4 at a maximum. This value is nearly equivalent to the concordance rate of 60% in the computer simulation result shown in Fig. 7 and indicates that the changes in the *SS* patterns and these physiological indices corresponded to each other two out of three times on average.

Furthermore, the values of I obtained for ρ_{max} and *RSA* were relatively higher at $L = \pm 1$ and $L = 0$, respectively, than at the other lag times. This result indicates that there was not much difference between the times the subjects experience VIMS symptoms and the times when their physiological state change. However, this tendency was not significant. This result may be caused by the limited number of subjects used to calculate the mean value of I for each lag time, which was approximately five or less, because there were significant individual differences in L_{max}. On the other hand, it is interesting to investigate the relationship between L_{max} and individual characteristics such as gender and age. Accordingly, data from more subjects is needed to make a statistically significant analysis for these relationships.

As shown in Fig. 10c, the maximum point of I obtained for *HRV* was not as high as those obtained for ρ_{max} or *RSA*. This result implies that indices obtained by the frequency or the correlated analysis of *HRV* can reflect the influence of VIMS on nervous activity more than *HRV* itself. On the other hand, the value of I obtained for LF_{HRV} was the lowest of all the $PS(k)$, and this result is considered to be reasonable because it is not clear whether LF_{HRV} reflect the development of VIMS. The difference between LF_{HRV} and *RSA* is considered to be associated with the difference in the autonomic nerve activity linked to these indices. Thus, *RSA* reflects parasympathetic nerve activity while LF_{HRV} is related to both sympathetic and parasympathetic nerve activities [33–35].

There was a minor difference in timing between ρ_{max} and *RSA* when the connection between *SS* and these physiological indices was strengthened. That is, the physiological reaction seen in *RSA* appeared at almost the same time the subjectivity evaluation changed, while the reaction in ρ_{max} appeared before or after the subjectivity evaluation changed, as shown in Figs. 9 and 10a. This latter result is of particular interest because it indicates that there were two types of subjects, whose reaction patterns of ρ_{max} differed from each other. In one type, the physiological states changed prior to the development of VIMS symptoms, while in the other type, the opposite was true. In the former case, the subjects had watched a scene which had the potential to induce VIMS and experienced changes to their physiological states. Then, approximately 1 min later, their emotional states changed. In the latter case, the possibility exists that the physiological states of the subjects changed as a result of the discomfort induced by VIMS. In this matter, the proposed method revealed that there were significant differences in the temporal relationship between physiological and emotional states among individuals.

In this study, it was necessary to establish a method to investigate not only the distribution of lag times but also the strength of the relationship between physiological and emotional states of subjects watching a video in considering their individual differences. The proposed method is considered to be an effective approach to accomplish our purpose. However, the values of I were not so high, which were less than 0.6, and no significant difference

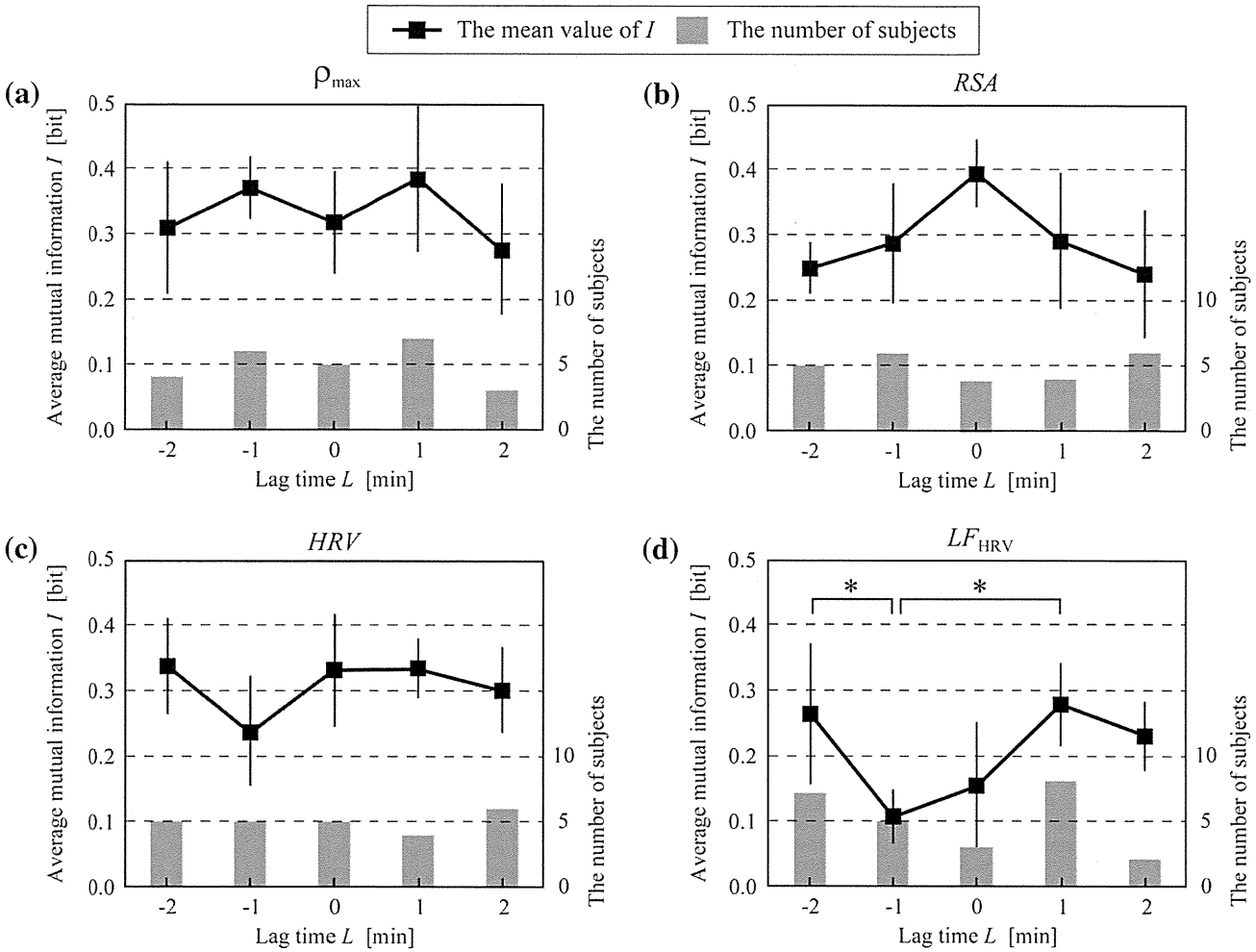

Fig. 10. The mean values of I between *SS* and four physiological indices: (a) ρ_{max}, (b) *HRV*, (c) LF_{HRV}, and (d) *RSA*. The bar graph at each lag time represents the number of subjects whose I was the highest at that lag time. $^{*}p < 0.05$, Tukey–Kramer test.

was found in the mean value of I between lag times for most physiological indices used in this study.

On the other hand, there is still room for improvement not only in the physiological indices but also in the subjective assessment method for the calculation of I. For example, by the use of techniques such as neural networks and genetic algorithms [36] with the AMI as a performance function, it may be possible to create a new index that can detect the development of VIMS with high accuracy. The continuous subjective assessment, in which subjects can report *SS* whenever they experience VIMS symptoms, may be useful to improve the proposed method. In the experiment of this study, the subjects reported *SS* by moving a joystick every time they heard a buzzer sound at 1 min intervals. This assessment method was designed to make certain subjects report their symptoms at least once a minute, however, there is a possibility to cause a delay, which is 1 min at worst, between the time subjects experience VIMS symptoms and that they change *SS*. On the other hand, even if the continuous subjective assessment is used, subjects do not always report *SS* just after they experience the symptoms because they may forget to report, and this becomes a serious problem for the calculation of AMI.

Information of video scenes related to VIMS cannot be obtained directly from the values of I nor L_{max}. As a first step to detect these scenes, it is necessary to find a physiological index that well reflects VIMS symptoms by calculating AMI as mentioned above. Then, it will be possible to find out which scenes in a video are associated with the onset of VIMS by analyzing the physiological index of subjects watching the video. In addition, if the physiological index has a tendency to change prior to feeling VIMS symptoms, it may be possible to predict the development of VIMS.

5. Conclusion

In this study, the AMI was employed to investigate the temporal relationship between subjective evaluation scores and collected physiological indices. Our analysis of experimental data suggested that changes in certain physiological indices showed a concordance rate of more than 60% with the change in the severity of VIMS symptoms. This result indicates that it may be possible to detect video scenes that are likely to induce VIMS by analyzing physiological indices. Furthermore, the physiological states of some test subjects changed prior to the development of VIMS symptoms, even though there were significant individual differences in the temporal relationship. An analysis of the temporal relationship between the physiological states and the cognitive levels of test subjects suffering from VIMS is expected to shed light on the pathogenesis of VIMS.

In our future work, analysis using other physiological indices, such as gastric tachyarrhythmia, which has frequently been reported as having a relationship with motion sickness, will be necessary. And our method using AMI should be compared to the

other techniques such as Cronbach's Alpha [37], which is a form of factor analysis. Furthermore, the number of sampling points used in this study might be insufficient for a full analysis of the AMI, so an experiment in which the video watching duration is extended, or where more subjects watch the same video repeatedly, should be performed to confirm the validity of the proposed method.

Acknowledgements

Dr. Hiroyasu Ujike and Dr. Atsuhiko Iijima provided excellent technical support in performing the experiment.

This study was subsidized by JKA through its Promotion funds from KEIRIN RACE and was supported by the Mechanical Social Systems Foundation and the Ministry of Economy, Trade and Industry of Japan.

References

[1] J.T. Reason, Motion sickness: some theoretical and practical considerations, Applied Ergonomics 9 (3) (1978) 163–167.
[2] N. Himi, T. Koga, E. Nakamura, M. Kobashi, M. Yamane, K. Tsujioka, Differences in autonomic responses between subjects with and without nausea while watching an irregularly oscillating video, Autonomic Neuroscience. Basic and Clinical 116 (2004) 46–53.
[3] N. Sugita, M. Yoshizawa, A. Tanaka, K. Abe, T. Yambe, S. Nitta, Evaluation of the effect of visual stimulation on humans by simultaneous experiment with multiple subjects, in: Proceedings of the 27th Annual International Conference of the IEEE Engineering in Medicine and Biology Society, 2005 (CD-ROM).
[4] N. Sugita, M. Yoshizawa, M. Abe, A. Tanaka, T. Yambe, S. Nitta, S. Chiba, Biphasic effect of visually-induced motion sickness revealed by time-varying correlation of autonomic nervous system, in: Proceedings of the tenth International Conference on Human – Computer Interaction, 2005 (CD-ROM).
[5] N. Sugita, M. Yoshizawa, M. Abe, A. Tanaka, T. Watanabe, S. Chiba, T. Yambe, S. Nitta, Evaluation of adaptation to visually induced motion sickness based on the maximum cross-correlation between pulse transmission time and heart rate, vol. 4(37), Journal of NeuroEngineering Rehabilitation (Online), 2007, <http://www.jneuroengrehab.com/content /4/1/35>.
[6] H. Ujike, K. Ukai, K. Nihei, Survey on motion sickness-like symptoms provoked by viewing a video movie during junior high school class, Displays 29 (2) (2008) 81–89.
[7] M. Emoto, M. Sugawara, Y. Nojiri, Viewing angle dependency of visually-induced motion sickness in viewing wide-field images by subjective and autonomic nervous indices, Displays 29 (2) (2008) 90–99.
[8] N. Sugita, M. Yoshizawa, A. Tanaka, K. Abe, S. Chiba, T. Yambe, S. Nitta, Quantitative evaluation of effects of visually-induced motion sickness based on causal coherence functions between blood pressure and heart rate, Displays 29 (2) (2008) 167–175.
[9] J.E. Bos, S.C. Vries, M.L. Emmerik, E.L. Groen, The effect of internal and external fields of view on visually induced motion sickness, Applied Ergonomics 41 (4) (2010) 516–521.
[10] J.T. Reason, J.J. Brand, Motion Sickness, Academic Press, London, 1975.
[11] J.T. Reason, Motion sickness adaptation: a neural mismatch model, Journal of the Royal Society of Medicine 71 (1975) 819–829.
[12] A.J. Benson, Motion sickness, in: M.R. Dix, J.S. Hood (Eds.), Vertigo, Wiley, New York, 1984, pp. 391–426.
[13] R.S. Kennedy, N.E. Lane, K.S. Berbaum, M.G. Lilienthal, Simulation sickness questionnaire: an enhanced method for quantifying simulator sickness, International Journal of Aviation Psychology 3 (3) (1993) 203–220.
[14] W.T. Lo, R.H.Y. So, Cybersickness in the presence of scene rotational movements along different axes, Applied Ergonomics 32 (1) (2001) 1–14.
[15] S. Nichols, H. Patel, Health and safety implications of virtual reality: a review of empirical evidence, Applied Ergonomics 33 (3) (2002) 251–271.
[16] S. Sharples, S. Cobb, A. Moody, J.R. Wilson, Virtual reality induced symptoms and effects (VRISE): comparison of head mounted display (HMD), desktop and projection display systems, Displays 29 (2) (2008) 58–69.
[17] R.S. Kennedy, J. Drexler, R.C. Kennedy, Research in visually induced motion sickness, Applied Ergonomics 40 (2010) 494–503.
[18] S.H.J. Uijtdehaage, R.M. Stern, K.L. Koch, Effects of eating on vection-induced motion sickness, cardiac vagal tone, and gastric myoelectric activity, Psychophysiology 29 (1992) 193–201.
[19] P.J. Gianaros, K.S. Quigley, E.R. Muth, M.E. Levine, R.C. Vasko Jr., R.M. Stern, Relationship between temporal changes in cardiac parasympathetic activity and motion sickness severity, Psychophysiology 40 (2003) 39–44.
[20] S. Hu, W.F. Grant, R.M. Stern, K.L. Koch, Motion sickness severity and physiological correlates during repeated exposures to a rotating optokineic drum, Aviation, Space, and Environmental Medicine 62 (1991) 308–314.
[21] J.C. Miller, T.J. Sharkey, G.A. Graham, M.E. McCauley, Autonomic physiological data associated with simulator discomfort, Aviation, Space, and Environmental Medicine 64 (9) (1993) 813–819.
[22] R.M. Stern, K.L. Koch, H.W. Leibowitz, I.M. Lindblad, C.L. Shupert, W.R. Stewart, Tachygastria and motion sickness, Aviation, Space, and Environmental Medicine 56 (1985) 1074–1077.
[23] B. Min, S. Chung, Y. Min, K. Sakamoto, Psychophysiological evaluation of simulator sickness evoked by a graphic simulator, Applied Ergonomics 35 (2004) 549–556.
[24] S. Cerutti, G. Baselli, A. Bianchi, M.G. Signorini, Spectral techniques of analysis for blood pressure and heart rate signals, Blood Pressure and Heart Rate Variability, IOS Press, Amsterdam, 1992.
[25] M. Pagani, L. Federico, G. Stefano, R. Ornella, F. Raffaellow, P. Paolo, S. Giulia, M. Gabriella, Power spectral analysis of heart rate and arterial pressure variabilities as a marker of sympatho-vagal interaction in man and conscious dog, Circulation Research 59 (1986) 178–193.
[26] G.B. Guo, M.D. Thames, F.M. Abboud, Arterial baroreflexes in renal hypertensive rabbits, Circulation Research 53 (1983) 223–234.
[27] T. Matsukawa, E. Gotoh, O. Hasegawa, H. Shionoiri, O. Tochikubo, M. Ishii, Reduced baroreflex changes in muscle sympathetic nerve activity during blood pressure elevation in essential hypertension, Journal of Hypertens 9 (1991) 537–542.
[28] S. Ogoh, J.P. Fisher, E.A. Dawson, M.J. White, N.H. Secher, P.B. Raven, Autonomic nervous system influence on arterial baroreflex control of heart rate during exercise in humans, Journal of Physiology 556 (2) (2005) 599–611.
[29] B. Gribbin, A. Steptoe, P. Sleight, Pulse wave velocity as a measure of blood pressure change, Psychophysiology 13 (1) (1976) 86–90.
[30] K. Jinzenji, H. Watanabe, N. Kobayashi, Global Motion Estimation for Sprite Production and Application to Video Coding (in Japanese), Information and Communication Engineers J83-D-II (2) (2000) 535–544.
[31] C.E. Shannon, The mathematical theory of communicaton, Bell System Technical Journal 27 (1948) 379–423.
[32] N. Tanaka, H. Okamoto, M. Naito, Detecting and evaluating intrinsic nonlinearity present in the mutual dependence between two variables, Physica D 147 (2000) 1–11.
[33] A. Malliani, M. Pagani, F. Lombardi, S. Cerutti, Cardiovascular neural regulation explored in the frequency domain, Circulation 84 (2) (1991) 482–492.
[34] G.G. Berntson, J.T. Bigger, D.L. Eckberg, P. Grossman, P.G. Kaufmann, M. Malik, H.N. Nagaraja, S.W. Porges, J.P. Saul, P.H. Stone, M.W. van derMolen, Heart rate variability: origins, methods, and interpretive caveats, Psychophysiology 34 (1997) 623–648.
[35] A. Malliani, N. Montaro, Heart rate variability as a clinical tool, Italian Heart Journal 3 (2002) 439–445.
[36] J.H. Holland, Adaptation in Natural and Artificial Systems: An Introductory Analysis with Applications to Biology, Control, and Artificial Intelligence, MIT Press, 1975.
[37] L.J. Cronbach, Coefficient alpha and the internal structure of tests, Psychometrika 16 (3) (1951) 297–334.